Published in final edited form as:
J Membr Biol. 2011 November ; 244(2): 81–91. doi:10.1007/s00232-011-9400-8.

Postnatal expression of an apamin-sensitive K(Ca) current in vestibular calyx terminals

Frances L. Meredith[1,2], **Gang Q. Li**[1,4], and **Katherine J. Rennie**[1,2,3]

[1]Department of Otolaryngology, University of Colorado at Anschutz Medical Campus, 12700 E. 19th Avenue, MS: 8606 Aurora, CO 80045

[2]Neuroscience Graduate Program, University of Colorado at Anschutz Medical Campus, 12700 E. 19th Avenue, MS: 8606 Aurora, CO 80045

[3]Department of Physiology & Biophysics, University of Colorado at Anschutz Medical Campus, 12700 E. 19th Avenue, MS: 8606 Aurora, CO 80045

Abstract

Afferent innervation patterns in the vestibular periphery are complex and vestibular afferents show a large variation in their regularity of firing. Calyx fibers terminate on type I vestibular hair cells and have firing characteristics distinct from bouton fibers that innervate type II hair cells. Whole cell patch clamp was used to investigate ionic currents that could influence firing patterns in calyx terminals. Underlying K(Ca) conductances have been described in vestibular ganglion cells, but their presence in afferent terminals has not been investigated previously. Apamin, a selective blocker of SK-type calcium-activated K^+ channels, was tested on calyx afferent terminals isolated from gerbil semicircular canals during postnatal days 1 to 50. Lowering extracellular calcium or application of apamin (20–500 nM) reduced slowly activating outward currents in voltage clamp. Apamin also reduced the action potential after-hyperpolarization (AHP) in whole cell current clamp, but only after the first two postnatal weeks. K^+ channel expression increased during the first postnatal month and SK channels were found to contribute to the AHP, which may in turn influence discharge regularity in calyx vestibular afferents.

Keywords

Afferent; After-hyperpolarization; Crista; Hair cell; Inner ear; Development

Introduction

Three afferent classes with different electrophysiological properties have been defined in the vestibular periphery of mammals (Baird et al. 1988; Fernández et al. 1988). Type I vestibular hair cells make synapses with encompassing afferent calyx terminals (calyx afferents), whereas smaller bouton fibers make synapses with type II hair cells only (bouton afferents). Dimorphic fibers constitute a third type of afferent class which receive input from both type I and type II hair cells. All three classes of afferent are spontaneously active and their discharge rate is modulated by deflections of the hair bundle, but individual afferent discharge regularity ranges from highly irregular to regular (Goldberg 2000). Calyx fibers

Correspondence to: K. Rennie, Department of Otolaryngology, 12700 E. 19th Avenue, MS: 8606 Aurora, Colorado 80045, Contact Telephone: 303 724 3070, Contact Fax: 303 724 1961, katie.rennie@ucdenver.edu.
[4]Present address: Department of Otology and Laryngology, Harvard Medical School, Eaton-Peabody Laboratories, Massachusetts Eye and Ear Infirmary, 243 Charles St., Boston, MA 02114

are relatively large in diameter and show irregular action potential discharge and phasic response dynamics. Bouton terminals are smaller in diameter, more regular in action potential firing and show tonic responses to acceleration, whereas dimorphic afferents show intermediate properties (Baird et al. 1988; Lysakowski et al. 1995). Recent whole cell patch clamp recordings from vestibular ganglion cells support the hypothesis that distinct membrane conductances contribute to different firing patterns (Iwasaki et al. 2008; Kalluri et al. 2010; Limón et al. 2005; Risner and Holt 2006). Regular afferents have more pronounced AHPs than irregular afferents which may arise due to the paucity of low voltage activated K^+ channels in regular neurons (Kalluri et al. 2010). Smith and Goldberg (1986) suggested that calcium-activated potassium (K(Ca)) channels might influence firing regularity in vestibular afferents, but to date this hypothesis has not been tested experimentally in identified afferents.

Vestibular afferents are bipolar neurons that make terminal synapses with hair cells in the crista ampullaris and otolith organs, have cell bodies in the vestibular ganglion and project to target neurons in the central nervous system. Several ionic conductances have been described in afferent cell bodies of isolated vestibular ganglia including voltage and calcium-gated K^+ currents (Chabbert et al. 2001a; Iwasaki et al. 2008; Kalluri et al. 2010; Limón et al. 2005; Risner and Holt 2006), hyperpolarization-activated current (I_h) (Chabbert et al. 2001b), sodium (Chabbert et al. 1997) and calcium currents (Autret et al. 2005; Chambard et al. 1999; Desmadryl et al. 1997). Although cell bodies in the ganglion have different diameters that are associated with certain electrophysiological characteristics, peripheral terminations are absent in these preparations (Iwasaki et al. 2008; Limón et al. 2005; Risner and Holt 2006). Therefore a clear segregation into calyx, bouton or dimorphic fibers has not been possible in studies of ganglion cell bodies. Although there are fewer reports of whole cell patch clamp recordings close to the hair cell/afferent synapse, recent recordings have revealed voltage-dependent conductances and action potentials in postsynaptic cochlear afferents (Curti et al. 2008; Glowatzki and Fuchs 2002; Weisz et al. 2009; Yi et al. 2010) and vestibular calyx afferents (Dhawan et al. 2010; Hurley et al. 2006; Rennie and Streeter 2006). Afferent boutons innervating inner hair cells in pre-hearing rats (P7–P14) and calyx terminals isolated from gerbil semicircular canals (P13–P84) expressed tetrodotoxin (TTX)-sensitive Na^+ conductances and 4-AP and TEA-sensitive outward K^+ conductances (Dhawan et al. 2010; Rennie and Streeter 2006; Yi et al. 2010). A mixed cation current, I_h, was also described in inner hair cell afferent terminals (Yi et al. 2010). To date K(Ca) conductances in mammalian inner ear afferent terminals have not been investigated. Therefore in this study we recorded from large unmyelinated calyx afferent endings on type I vestibular hair cells to determine the biophysical properties of K(Ca) currents in calyx fibers and to investigate the role of K(Ca) channels in development and action potential shaping.

Materials and methods

Cell isolation

Experiments were performed on Mongolian gerbils of both sexes at postnatal days (P)1-P50 under protocols approved by the University of Colorado's Institutional Animal Care and Use Committee. Gerbils were injected with pentobarbital sodium (Nembutal, 50 mg/kg intraperitoneal) and ketamine (10 mg/kg intramuscular). The vestibular system was removed under deep anesthesia prior to decapitation. Type I hair cells along with their calyx terminals were isolated as described previously (Dhawan et al. 2010). Briefly, ampullae were immersed in a solution containing (in mM): NaCl (135), KCl (5), $MgCl_2$ (10), $CaCl_2$ (0.02), HEPES (10) and D-glucose (3), pH 7.4 with NaOH and osmolality 300–305 mmol/kg for 30 to 32 minutes at 37 C and then transferred to Leibovitz's L-15 medium with bovine albumin (0.5 mg/ml) for a minimum of 50 minutes at room temperature (21–24 C). A fine probe was

used to make furrows along individual cristae immersed in standard L-15 medium (osmolality adjusted to 300–305 mmol/kg with distilled H_2O, pH 7.4–7.6) thereby mechanically dissociating cells from the neuroepithelium. Cells were observed on an Olympus upright microscope (BX50 or BX51WI) with a 40X water immersion objective and IR differential interference contrast optics. Type I hair cells were identified by their characteristic amphora shape and recordings were made from afferent calyx terminals that remained attached to the basolateral regions of type I hair cells as described previously (Dhawan et al. 2010; Rennie and Streeter 2006).

Electrophysiological recording and solutions

A horizontal micropipette puller (Sutter Instruments, San Rafael, CA) was used to pull patch pipettes from glass capillaries (Warner Instrument Corp., Hamden, CT, glass PG165T, outer diameter 1.65 mm, inner diameter 1.28 mm). Pipettes were fire-polished on a microforge (Narishige MF 830) before coating with silicone elastomer (Sylgard, Dow Corning, Midland MI). The patch pipette solution used in the majority of experiments was (in mM): potassium fluoride (KF) (110), KCl (15), NaCl (1), HEPES (10), D-glucose (3), $MgCl_2$ (1.8), EGTA (10), MgATP (2) and Li_xGTP (0.2), pH 7.4 with KOH (~ 27 mM) but was KF (100), KCl (20), K-gluconate (28), NaCl (2), HEPES (10), D-glucose (3), $MgCl_2$ (2) and EGTA (10), pH 7.4 with KOH (24 mM) in the amlodipine experiments. To record inward calcium currents electrode K^+ was replaced with Cs^+.

Patch pipette resistance was 1 – 5 MΩ and pipette tips were placed on the outer face of the calyx membrane to form gigaseals. All recordings described here were from calyx endings enclosing a single type I hair cell. Following membrane rupture, whole cell patch clamp recordings were carried out in voltage or current clamp at room temperature (21–24ºC). Currents were amplified with an Axopatch 200B or Axopatch-1D patch amplifier (Molecular Devices, Sunnyvale, CA) interfaced to a PC running PClamp (v 8 or 10) through an AD converter (Digidata 1320A or 1440A Molecular Devices). Data were filtered at 5 kHz and sampled at a minimum of 10 kHz. Capacitance was compensated electronically. Corrections for liquid junction potentials were made during data analysis.

We typically observed an increase (run up) of sodium current (I_{Na}) and a decrease (run down) in the macroscopic outward potassium current (I_K) in calyx terminals during the first few minutes of whole cell recording. Following membrane breakthrough, peak outward current, measured at a step to +20 mV, decreased on average by 1.4 % per minute in control whole cell recordings held between 8 and 27 minutes (1.36 ± 0.20 %, mean ± SEM, n = 11). Input resistance also increased significantly (P = 0.006, paired t-test) from 994 ± 96 MΩ to 1669 ± 220 MΩ (mean ± SEM, n = 9 cells) during the first few minutes following membrane rupture.

AHP size was calculated by taking the difference between the maximum hyperpolarization to depolarization following the action potential. AHP measurements were taken from 5 action potentials averaged during controls and 5 action potentials averaged following drug application for each cell.

Chemicals were obtained from Sigma-Aldrich (St Louis, MO), except for apamin which was obtained from Tocris Bioscience (Ellisville, MO) and amlodipine obtained from Enzo Life Sciences (Plymouth, PA). Stock solutions of apamin were made up in distilled water and stored at −20ºC before final dilution in L-15. Amlodipine stock solutions were made up in DMSO and stored at −20ºC before diluting in L-15 (< 0.001 % final DMSO concentration). Low Ca^{2+} solution contained no added Ca^{2+} (nominally 0 mM Ca^{2+}) and consisted of (in mM): NaCl (140), KCl (5), $MgCl_2$ (3.1), HEPES (10) and D-glucose (3), pH 7.4 with NaOH and replaced a similar solution (normal HEPES solution) containing 1.3 $CaCl_2$ and 1.8 mM

$MgCl_2$. Cadmium solution was normal HEPES solution to which was added 0.1 mM $CdCl_2$. The recording chamber was perfused using a peristaltic pump at a flow rate of between 0.5–1 ml/minute. Drugs were applied locally from a perfusion device with 3 inlets into a common outlet, or from a pneumatic Picopump (PV820, WPI, Sarasota, Florida) or by rapidly replacing the bath solution using a transfer pipette. TTX (500 nM) was added to the extracellular solution in some recordings to block I_{Na}.

Results

Lowering extracellular Ca^{2+} reduces outward currents in calyx afferent terminals

Previous studies have identified different voltage-gated K^+ channels in calyx afferent terminals based on sensitivities to tetraethylammonium (TEA), 4-aminopyridine (4-AP) and the KCNQ channel blockers XE991 and linopirdine (Dhawan et al. 2010; Hurley et al. 2006; Rennie and Streeter 2006). Fig. 1A demonstrates typical voltage-dependent I_{Na} and outward K^+ currents in calyces in response to a 40 ms hyperpolarizing voltage step followed by a series of depolarizations. In response to longer duration pulses (640 ms) from a holding potential of −79 mV, a slowly activating inward current is apparent at hyperpolarized potentials. This current strongly resembles a hyperpolarization-activated and cyclic nucleotide-gated (HCN) current as previously described in vestibular ganglion neurons and auditory afferents (Chabbert et al. 2001b; Yi et al. 2010).

K(Ca) conductances in afferent terminals have not been investigated previously. To determine whether the outward current had a Ca^{2+}-dependent component, external Ca^{2+} was removed during whole cell recordings (Fig. 2). Fig. 2A shows the response of a calyx to repeated applications of nominally zero Ca^{2+} solution during a depolarizing voltage step. Peak outward currents were reduced in response to successive applications of low Ca^{2+} solution and demonstrated partial recovery between applications (Fig. 2A). Examples of control current, showing an initial transient inward Na^+ current followed by outward K^+ current, and current in low Ca^{2+} solution are shown in Fig. 2B. The slowly activating outward current reduced in low Ca^{2+} was obtained by subtraction and is shown in Fig. 2B (dashed line). Similar results were seen in cells at ages between P14 and P22, with low Ca^{2+} application producing a mean reduction of 20.6 ± 4.6 % (mean ± SEM, n = 8) in peak outward current. Currents measured at the end of the voltage step in control conditions and following low Ca^{2+} perfusion, in addition to the Ca^{2+}-sensitive component (triangles) are shown at different voltages in Fig. 2C.

We investigated the presence of Ca^{2+} currents that could underlie the K(Ca) current. Transient T-type Ca^{2+} currents have been described in embryonic vestibular ganglion neurons where they contribute to spiking activity (Autret et al. 2005). We have previously recorded transient inward currents in gerbils aged 3 weeks and older, which were ~ 80 % blocked by the Na^+ channel blocker TTX (100 nM) (Rennie and Streeter 2006). In further experiments we recorded transient inward currents in early postnatal calyces between P1 and P24. Rapid inward currents were completely blocked by 500 nM tetrodotoxin as shown for a P8 calyx in Fig. 3A, B. We found that 500 nM tetrodotoxin reduced peak transient inward currents in calyces aged P8–P24 by 96.3 ± 1.0 % (mean ± SEM, n = 20 cells), confirming that transient inward currents in postnatal calyces at these ages are due to TTX-sensitive Na^+ channels and not T-type Ca^{2+} channels.

L-type Ca^{2+} channels have been implicated in regulating neuronal excitability by coupling to K(Ca) and non-specific cation channels mediating AHPs in hippocampal neurons (Geier et al. 2011). L-type Ca^{2+} currents were described in isolated vestibular ganglion neurons in P4–P8 mice (Desmadryl et al. 1997). We investigated the effects of the Ca^{2+} channel antagonists amlodipine and nifedipine on K^+ currents in calyces and found a marked

reduction in outward current in response to extracellular application of both antagonists (Fig. 4A-C). Amlodipine blocked a slowly activating current as shown in Fig. 3A and the amlodipine-sensitive current activated above −40 mV (Fig. 4B). In 13 cells (ages P21 to P50) the outward current at the end of a voltage step to +20 mV was reduced by an average of 34.3 ± 4.6 % in 7 μM amlodipine. The effect was partially reversible in 6 cells. A similar effect was seen with the selective dihydropyridine L-type Ca^{2+} channel antagonist nifedipine (Fig. 4C). Outward current at the end of the voltage step was decreased by an average of 27.4 ± 8.9 % (n = 3, P33) by 20 μM nifedipine.

To investigate inward Ca^{2+} currents, electrode K^+ was replaced with Cs^+ to reduce outward currents. Under these conditions small amplitude, slowly activating inward currents could be recorded at potentials above −40 mV, which were greatly reduced by application of the broad spectrum Ca^{2+} channel blocker cadmium (Fig. 4D). As shown in Fig. 4D, 0.1 mM Cd^{2+} did not block the transient inward Na^+ current, but reduced the slow inward current during a depolarizing voltage step. The simplest interpretation of these results is that the slow inward current results from voltage-dependent Ca^{2+} channels, which at depolarized membrane potentials could lead to Ca^{2+} entry and activation of nearby K(Ca) channels.

Apamin block of outward current

Primary vestibular afferents project to the vestibular ganglion and ganglion cell bodies express K(Ca) currents with different underlying K(Ca) channels (Limón et al. 2005). Are K(Ca) channels also expressed on calyx terminals? To further probe the nature of the Ca^{2+}-sensitive outward current in calyx terminals we applied apamin, a component of bee venom which selectively blocks small conductance (SK) channels (Sah and Faber 2002). In 16/20 cells (ages P13–P26) apamin (100 nM) produced a reduction in outward currents when applied extracellularly. Average reduction of the peak outward currents in 100 nM apamin was 32.5 ± 4.4 % (n = 16) and the effect was partly reversible in 8 cells. Fig. 5 shows the effect of apamin on outward currents in a P24 calyx terminal. Control outward currents showed a small amount of inactivation during a 40 ms test step, but following apamin application at 20 and 100 nM, inactivation of outward currents became more pronounced (Fig. 5A). Subtracting the residual current in 100 nM apamin from control current revealed that the apamin-sensitive component (dashed line) was slowly activating (Fig. 5A). The apamin-sensitive component therefore has a similar kinetic profile to the current blocked by lowering extracellular Ca^{2+} (Fig. 2B), the current blocked by dihydropyridines (Fig. 4A-C) and a TEA-sensitive current (I_{TEA}) that we have described previously (Dhawan et al. 2010). The IV plot in Fig. 5B shows control currents, currents following the two different concentrations of apamin and recovery following drug washout. SK channels are voltage-independent and are activated by increases in cytosolic Ca^{2+}, however Ca^{2+} influx through Ca^{2+} channels is voltage-sensitive and voltage dependence of the outward current is presumably a reflection of this.

Apamin had no effect on outward currents in 3 type I vestibular hair cells tested (1 cell at P15 and 2 cells at P24, data not shown), confirming previous observations that these cells do not express significant SK channel activity (Rennie and Correia 1994; Rüsch and Eatock 1996).

Development of action potentials

We have previously reported that calyx terminals isolated from gerbils aged 3 weeks and older do not fire spontaneous action potentials, but single action potentials can be evoked in whole cell current clamp (Dhawan et al. 2010; Rennie and Streeter 2006). Maturation of the vestibular system occurs during the first postnatal month in rodents and includes electrophysiological changes in afferent firing patterns (Curthoys 1979, 1982). Type I

vestibular hair cells also show dramatic changes in their electrophysiological membrane properties during the first few postnatal weeks (Eatock and Hurley 2003; Hurley et al. 2006; Li et al. 2010), but little is known about the ionic currents that may underlie changes in excitability in postnatal afferents. We recorded I_{Na} and I_K in voltage clamp and action potentials in current clamp in isolated calyx terminals at postnatal ages P1 to P38. Although most calyces showed single action potentials, in some cases up to 3 successive spikes could be evoked. Examples of single action potentials at P1, P7, P13 and P27 in response to depolarizing current pulses following membrane hyperpolarization are shown in Fig. 6A. A prominent AHP was not present at P1 and P7, suggesting that the ion channels responsible for setting up the AHP were not functionally available at these early stages. By P14 most calyces (5 out of 6 studied) demonstrated an AHP after the spike and at P38, 3 out of 3 calyces studied showed an AHP (data not shown). Corresponding whole cell currents in voltage clamp from a P1 calyx and a P27 calyx are also shown (Fig. 6B) and normalized outward currents for calyces at three different postnatal ages are shown in Fig. 6C. Large Na^+ currents were present from P1 onwards (Fig. 6B). At P1 Na^+ currents ranged from 5–11 nA in peak amplitude in 4 calyces studied. In contrast, K^+ currents were typically small in magnitude during the first few days postnatally and increased in size during the first postnatal month (Fig. 6C). Current density was estimated by dividing peak I_K amplitude by calyx capacitance and averaged 175 ± 30 pA/pF at P1 (mean ± SEM, n = 3) and 1701 ± 336 pA/pF (n = 9) at P27. Therefore outward K^+ current density was on average almost 10 times greater at the end of the first postnatal month and the values were statistically significantly different at these two developmental ages ($P < 0.05$). Data suggest that the increase in outward K^+ current that occurs with postnatal development is associated with greater repolarization of the action potential and generation of the AHP following the action potential.

Effect of apamin on the voltage response to current pulses

We investigated the effect of apamin on action potentials in current clamp at ages P16–P24. Fig. 6D shows the effect of 100 nM apamin on a P16 calyx. In 6 cells tested, apamin (100 nM in 4 cells, 500 nM in 2 cells) slowed the falling phase of the action potential and resulted in a slow depolarization of the cell membrane during current injection compared to controls. In 5/6 cells the size of the AHP decreased (mean decrease per cell ranged from 1.6 to 4.4 mV) and the response showed a partial recovery during washout (Fig. 6D). The effects of apamin on the voltage response are consistent with block of the slowly activating outward SK current and strongly suggest that SK contributes to the AHP in these cells under our recording conditions.

Discussion

We describe here for the first time K^+ currents in calyx terminals in the vestibular periphery which are sensitive to apamin and external calcium removal and can therefore be identified as SK currents. The SK current described here has relatively slow activation kinetics in voltage clamp, activates above −40 mV, shows no evidence of inactivation, and is therefore similar to SK currents described in vestibular ganglion cells (Limón et al. 2005) and in inner hair cells (Marcotti et al. 2004). In current clamp, blocking SK channels slows the repolarizing membrane potential trajectory and decreases the size of the AHP following an action potential.

Other K^+ conductances in calyx terminals

We have previously identified two voltage-dependent outward K^+ currents in mature calyx terminals (Dhawan et al. 2010). The first current had rapid activation and inactivation kinetics and was blocked by 4-aminopyridine (4-AP) and the Kv3 channel blocker BDS-I.

The second current activated and inactivated with slower kinetics and was sensitive to TEA (30 mM) (Dhawan et al. 2010). Calcium-activated K^+ currents in calyx terminals were not investigated previously, but since SK channels are blocked by low concentrations of TEA (Monaghan et al. 2004); it is likely that part of the TEA-sensitive current described previously was due to SK current. M-like KCNQ channels may also contribute to the macroscopic outward current in mature and developing calyces. A K^+ current sensitive to the KCNQ channel blockers linopirdine and XE991 has been described in calyx terminals (Hurley et al. 2006; Rennie and Streeter 2006) and KCNQ4 immunoreactivity has been reported in rodent calyces (Hurley et al. 2006; Lysakowski et al. 2011; Rocha-Sanchez et al. 2007). Calmodulin can bind to the C terminus of KCNQ channels and increases in intracellular Ca^{2+} can mediate a Ca^{2+} dependent inhibition of M current through this interaction in a reconstituted system (Gamper and Shapiro 2003). Differential modulation of KCNQ4 variants by calmodulin has also been reported, however it is not known if Ca^{2+} regulates native KCNQ4 channels in hair cells (Xu et al. 2007).

Development and firing regularity of vestibular afferents

A small AHP is present following the action potential in many calyx terminals at 2 weeks and older. In other neurons, AHP conductances have been shown to play a role in setting firing rate, regularity and spike timing precision. During the fast repolarizing phase (downstroke) of the action potential, rapid K^+ channels such as BK, M channels and A-type channels contribute (Bean 2007). We have previously shown that 4-AP application increased action potential width, consistent with a repolarizing role of a rapid A-type conductance (Dhawan et al. 2010). TEA blocked a slower outward K^+ conductance in voltage clamp and in current clamp increased the width and reduced the amount of repolarization of the action potential (Dhawan et al. 2010). In experiments described here, apamin reduced both the action potential repolarization and AHP size. SK channels therefore contribute to the AHP in calyces, but in the absence of repetitive firing a precise role for SK in determining firing properties of calyx afferents remains speculative.

Regular and irregular firing patterns of primary vestibular afferents in mature vertebrates have been studied extensively using sharp electrode recordings (Goldberg 2000). Calyx afferents have the most irregular firing pattern and for most frequencies tested the sensitivity to head rotations is greater in irregular afferents than regular afferents (Hullar et al. 2005). The size and duration of AHPs may determine discharge regularity and a theoretical study suggested that vestibular afferents with smaller and faster AHPs would show irregular discharges (Smith and Goldberg 1986). However, little is known physiologically about the ionic conductances underlying discharge characteristics in peripheral vestibular afferents and their developmental regulation. In the vestibular system of rodents, afferent spontaneous activity is low in the embryonic period and increases gradually postnatally (Curthoys 1979, 1982; Desmadryl et al. 1986; Eatock and Hurley 2003). Regular firing patterns appear in rat semicircular canal afferents during the first postnatal week and both the rate and gain of firing increase during the first postnatal month (Curthoys 1979, 1982). It seems likely that not only developing ionic conductances in hair cells (Eatock and Hurley 2003; Li et al. 2010), but also afferent terminals contribute to these changes. Our results suggest that large Na^+ currents are present as early as P1 in calyx terminals, but that K^+ currents are relatively small at P1 and increase in size postnatally.

Comparison of calyx terminals to vestibular ganglion cells

Vestibular afferent fibers terminating in calyx, bouton and dimorphic endings project to cell bodies in the vestibular ganglion. Several voltage-gated and calcium-activated K^+ currents have been described in prenatal and early postnatal mammalian vestibular ganglion cells (Chabbert et al. 2001a, 2001b; Chambard et al. 1999; Iwasaki et al. 2008; Kalluri et al. 2010;

Limón et al. 2005; Pérez et al. 2009; Risner and Holt 2006). K(Ca) currents in rat vestibular ganglion soma were reported to have underlying channels of high conductance (BK), intermediate conductance (IK) and small conductance (SK). These components were blocked by iberiotoxin, clotrimazole and apamin respectively and an additional K(Ca) component resistant to blockers was also described (Limón et al. 2005). BK channels contributed to neuronal discharge by repolarizing the action potential and influencing spike duration and BK current was more prominent in neurons with low-voltage activated Ca^{2+} currents (Limón et al. 2005). However, a recent immunocytochemical study found no evidence for BK channels in rat vestibular ganglion cells or afferent terminals, but instead reported BK channel staining in a minority of hair cells in the utricle and horizontal crista. Most BK-positive hair cells were innervated by a calretinin-positive calyx (Schweizer et al. 2009). Our results suggest that SK channels underlie the K(Ca) current component and play a role in determining the AHP in calyces. This differs from results in the cultured rat ganglion, where apamin and clotrimazole had no significant effect on action potential shape. However, those experiments were carried out in early postnatal (P7–P10) ganglia in the presence of 10 mM extracellular 4-AP, which may have influenced action potential characteristics (Limón et al. 2005). In contrast in inner hair cells an SK current was reported to be required for repolarization and repetitive firing in early postnatal days (Marcotti et al. 2004).

Embryonic mouse vestibular ganglion neurons fire single Na^+-dependent spikes and a fast activating, fast inactivating T-type Ca^{2+} current was found to contribute to an after depolarizing potential (ADP) (Autret et al. 2005). Thirty per cent of embryonic neurons also exhibited an AHP, but the underlying channels were not investigated. The low voltage activated T-type current in mouse ganglion neurons decreased with development and was virtually absent at birth (Autret et al. 2005). However rat cultured vestibular ganglion neurons (ages P7–P10) expressed both low- (T-type) and high-voltage activated inward calcium currents (Limón et al. 2005). We found no evidence for a T-type Ca^{2+} current in postnatal calyx terminals, which is consistent with a lack of Cav3.1 immunoreactivity in afferent terminals in early postnatal mouse saccule and crista (Nie et al. 2008). The transient inward current in calyx terminals aged P8–P24 was blocked > 95 % by 500 nM tetrodotoxin (Fig. 3), confirming it was a Na^+ conductance. TTX-sensitive Na^+ currents have also been reported in mouse vestibular ganglia aged P3 to P6 (Chabbert et al. 1997) and in rat inner hair cell afferent dendrites at ages P7–P14 (Yi et al. 2010). A slow and sustained cadmium-sensitive Ca^{2+} current may mediate Ca^{2+} entry necessary to activate SK channels in calyces (Fig. 4D) and we found a dihydropyridine-sensitive component of the outward calyceal K^+ current activating above −40 mV (Fig. 4A-C) suggesting dihydropyridines blocked Ca^{2+} entry through voltage-gated L-type Ca^{2+} channels. The coupling between inward Ca^{2+} flux and SK current in calyces warrants further study.

Functional role of K(Ca) channels

The underlying mechanisms governing firing in vestibular afferents are not well understood. If K(Ca) channels play a role in regulating firing, altering internal Ca^{2+} levels would modulate K(Ca) channel activity. In gerbil vestibular epithelia calretinin is restricted to calyx-only afferents (Leonard and Kevetter 2002) and this calcium-binding protein may be involved in regulating cytosolic Ca^{2+} levels. Based on the similar molar range of the K_d for binding Ca^{2+} to calretinin and for activating SK channels, it has been suggested that calretinin could reduce Ca^{2+} availability to SK channels and decrease channel activation, contributing to the irregular discharge pattern found in calretinin-containing calyx afferents (Desai et al. 2005). In patch clamp recordings from calyces and ganglion cell bodies spontaneous action potentials are not typically observed and therefore discharge regularity cannot be measured. However, we found an effect of apamin on evoked single action

potentials in calyces and further studies in more intact preparations, where connections to hair cells and ganglion are preserved, should elucidate the role of SK in discharge regularity in primary vestibular afferents. Interestingly BK null mutant mice have no obvious vestibular deficits (Pyott et al. 2007), but an SK mutant shows locomotion problems that may be linked to disruption of vestibular processing (Szatanik et al. 2008). Although deficits in this mutant may arise due to lack of functional central SK channels, which have been demonstrated in vestibular nucleus neurons (Dutia and Johnston 1998; Saito et al. 2008; Smith et al. 2002), our results suggest that SK channels in vestibular calyces may also play an important role in the peripheral processing of vestibular signals.

Acknowledgments

This work was supported by National Institute on Deafness and other Communication Disorders (NIDCD) Grant DC-008297 and an American Otological Society Grant to KJR. FLM was partly supported by 5T32NS007083. We thank Tommy Bui for excellent technical help and Scott Mann for comments on the manuscript.

References

Autret L, Mechaly I, Scamps F, Valmier J, Lory P, Desmadryl G. The involvement of $Ca_V3.2/\alpha1H$ T-type calcium channels in excitability of mouse embryonic primary vestibular neurons. J Physiol. 2005; 567:67–78. [PubMed: 15961427]

Baird RA, Desmadryl G, Fernández C, Goldberg JM. The vestibular nerve of the chinchilla. II. Relation between afferent response properties and peripheral innervation patterns in the semicircular canals. J Neurophysiol. 1988; 60:182–203. [PubMed: 3404216]

Bean BP. The action potential in mammalian central neurons. Nat Rev Neurosci. 2007; 8:451–465. [PubMed: 17514198]

Chabbert C, Chambard JM, Valmier J, Sans A, Desmadryl G. Voltage-activated sodium currents in acutely isolated mouse vestibular ganglion neurones. Neuroreport. 1997; 8:1253–1256. [PubMed: 9175124]

Chabbert C, Chambard JM, Sans A, Desmadryl G. Three types of depolarization-activated potassium currents in acutely isolated mouse vestibular neurons. J Neurophysiol. 2001a; 85:1017–1026. [PubMed: 11247971]

Chabbert C, Chambard JM, Valmier J, Sans A, Desmadryl G. Hyperpolarization-activated (Ih) current in mouse vestibular primary neurons. Neuroreport. 2001b; 12:2701–2704. [PubMed: 11522951]

Chambard JM, Chabbert C, Sans A, Desmadryl G. Developmental changes in low and high voltage-activated calcium currents in acutely isolated mouse vestibular neurons. J Physiol. 1999; 518:141–149. [PubMed: 10373696]

Curthoys IS. The development of function of horizontal semicircular canal primary neurons in the rat. Brain Res. 1979; 167:41–52. [PubMed: 455071]

Curthoys IS. Postnatal developmental changes in the response of rat primary horizontal semicircular canal neurons to sinusoidal angular accelerations. Exp Brain Res. 1982; 47:295–300. [PubMed: 7117454]

Curti S, Gómez L, Budelli R, Pereda AE. Subthreshold sodium current underlies essential functional specializations at primary auditory afferents. J Neurophysiol. 2008; 99:1683–1699. [PubMed: 18234982]

Desai SS, Zeh C, Lysakowski A. Comparative morphology of rodent vestibular periphery. I. Saccular and utricular maculae. J Neurophysiol. 2005; 93:251–266. [PubMed: 15240767]

Desmadryl G, Raymond J, Sans A. In vitro electrophysiological study of spontaneous activity in neonatal mouse vestibular ganglion neurons during development. Brain Res. 1986; 390:133–136. [PubMed: 3948026]

Desmadryl G, Chambard JM, Valmier J, Sans A. Multiple voltage-dependent calcium currents in acutely isolated mouse vestibular ganglion neurons. Neuroscience. 1997; 78:511–22. [PubMed: 9145806]

Dhawan R, Mann SE, Meredith FL, Rennie KJ. K^+ currents in isolated vestibular afferent calyx terminals. J Assoc Res Otolaryngol. 2010; 11:463–476. [PubMed: 20407915]

Dutia MB, Johnston AR. Development of action potentials and apamin-sensitive after-potentials in mouse vestibular nucleus neurons. Exp Brain Res. 1998; 118:148–154. [PubMed: 9547083]

Eatock RA, Hurley KM. Functional development of hair cells. Current Topics in Developmental Biology. 2003; 57:389–448. [PubMed: 14674488]

Fernández C, Baird RA, Goldberg JM. The vestibular nerve of the chinchilla. I. Peripheral innervation patterns in horizontal and superior semicircular canals. J Neurophysiol. 1988; 60:167–181. [PubMed: 3404215]

Gamper N, Shapiro MS. Calmodulin mediates Ca^{2+}-dependent modulation of M-type K^+ channels. J Gen Physiol. 2003; 122:17–31. [PubMed: 12810850]

Geier P, Lagler M, Boehm S, Kubista H. Dynamic interplay of excitatory and inhibitory coupling modes of neuronal L-type calcium channels. Am J Physiol. 2011; 300:C937–949.

Glowatzki E, Fuchs PA. Transmitter release at the hair cell ribbon synapse. Nat Neurosci. 2002; 5:147–154. [PubMed: 11802170]

Goldberg JM. Afferent diversity and the organization of central vestibular pathways. Exp Brain Res. 2000; 130:277–297. [PubMed: 10706428]

Hullar TE, Della Santina CC, Hirvonen T, Lasker DM, Carey JP, Minor LB. Responses of irregularly discharging chinchilla semicircular canal vestibular-nerve afferents during high-frequency head rotations. J Neurophysiol. 2005; 93:2777–2786. [PubMed: 15601735]

Hurley KM, Gaboyard S, Zhong M, Price SD, Wooltorton JRA, Lysakowski A, Eatock RA. M-like K^+ currents in type I hair cells and calyx afferent endings of the developing rat utricle. J Neurosci. 2006; 40:10253–10269. [PubMed: 17021181]

Iwasaki S, Chihara Y, Komuta Y, Ito K, Sahara Y. Low-voltage-activated potassium channels underlie the regulation of intrinsic firing properties of rat vestibular ganglion cells. J Neurophysiol. 2008; 100:2192–2204. [PubMed: 18632889]

Kalluri R, Xue J, Eatock RA. Ion channels set spike timing regularity of mammalian vestibular afferent neurons. J Neurophysiol. 2010; 104:2034–2051. [PubMed: 20660422]

Leonard RB, Kevetter GA. Molecular probes of the vestibular nerve. I Peripheral termination patterns of calretinin, calbindin and peripherin containing fibers. Brain Res. 2002; 928:8–17. [PubMed: 11844467]

Li G, Meredith FL, Rennie KJ. Development of K^+ and Na^+ conductances in rodent postnatal semicircular canal type I hair cells. Am J Physiol. Regul Integr Comp Physiol. 2010; 298:R351–8.

Limón A, Pérez C, Vega R, Soto E. Ca^{2+}-activated K^+-current density is correlated with soma size in rat vestibular-afferent neurons in culture. J Neurophysiol. 2005; 94:3751–3761. [PubMed: 16107534]

Lysakowski A, Minor LB, Fernández C, Goldberg JM. Physiological identification of morphologically distinct afferent classes innervating the cristae ampullares of the squirrel monkey. J Neurophysiol. 1995; 73:1270–1281. [PubMed: 7608770]

Lysakowski A, Gaboyard-Niay S, Calin-Jageman I, Chatlani S, Price SD, Eatock RA. Molecular microdomains in a sensory terminal, the vestibular calyx ending. J Neurosci. 2011; 31:10101–10114. [PubMed: 21734302]

Marcotti W, Johnson SL, Kros CJ. A transiently expressed SK current sustains and modulates action potential activity in immature mouse inner hair cells. J Physiol. 2004; 560:691–708. [PubMed: 15331671]

Monaghan AS, Benton DC, Bahia PK, Hosseini R, Shah YA, Haylett DG, Moss GW. The SK3 subunit of small conductance Ca^{2+}-activated K^+ channels interacts with both SK1 and SK2 subunits in a heterologous expression system. J Biol Chem. 2004; 279:1003–1009. [PubMed: 14559917]

Nie L, Zhu J, Gratton MA, Liao A, Mu KJ, Nonner W, Richardson GP, Yamoah EN. Molecular identity and functional properties of a novel T-type Ca^{2+} channel cloned from the sensory epithelia of the mouse inner ear. J Neurophysiol. 2008; 100:2287–2299. [PubMed: 18753322]

Pérez C, Limón A, Vega R, Soto E. The muscarinic inhibition of the potassium M-current modulates the action-potential discharge in the vestibular primary-afferent neurons of the rat. Neuroscience. 2009; 158:1662–1674. [PubMed: 19095045]

Pyott SJ, Meredith AL, Fodor AA, Vázquez AE, Yamoah EN, Aldrich RW. Cochlear function in mice lacking the BK channel alpha, beta1, or beta4 subunits. J Biol Chem. 2007; 282:3312–24. [PubMed: 17135251]

Rennie KJ, Correia MJ. Potassium currents in mammalian and avian isolated type I semicircular canal hair cells. J Neurophysiol. 1994; 71:317–329. [PubMed: 8158233]

Rennie KJ, Streeter MA. Voltage-dependent currents in isolated vestibular afferent calyx terminals. J Neurophysiol. 2006; 95:26–32. [PubMed: 16162827]

Risner JR, Holt JR. Heterogeneous potassium conductances contribute to the diverse firing properties of postnatal mouse vestibular ganglion neurons. J Neurophysiol. 2006; 96:2364–2376. [PubMed: 16855108]

Rocha-Sanchez SMS, Morris KA, Kachar B, Nichols D, Fritzsch B, Beisel KW. Developmental expression of Kcnq4 in vestibular neurons and neurosensory epithelia. Brain Res. 2007; 1139:117–125. [PubMed: 17292869]

Rüsch A, Eatock RA. A delayed rectifier conductance in type I hair cells of the mouse utricle. J Neurophysiol. 1996; 76:995–1004. [PubMed: 8871214]

Sah P, Faber ES. Channels underlying neuronal calcium-activated potassium currents. Prog Neurobiol. 2002; 66:345–353. [PubMed: 12015199]

Saito Y, Takazawa T, Ozawa S. Relationship between afterhyperpolarization profiles and the regularity of spontaneous firings in rat medial vestibular nucleus neurons. Eur J Neurosci. 2008; 28:288–298. [PubMed: 18702700]

Schweizer FE, Savin D, Luu C, Sultemeier DR, Hoffman LF. Distribution of high-conductance calcium-activated potassium channels in rat vestibular epithelia. J Comp Neurol. 2009; 517:134–45. [PubMed: 19731297]

Smith CE, Goldberg JM. A stochastic afterhyperpolarization model of repetitive activity in vestibular afferents. Biol Cybern. 1986; 54:41–51. [PubMed: 3487348]

Smith MR, Nelson AB, Du Lac S. Regulation of firing response gain by calcium-dependent mechanisms in vestibular nucleus neurons. J Neurophysiol. 2002; 87:2031–2042. [PubMed: 11929921]

Szatanik M, Vibert N, Vassias I, Guénet JL, Eugène D, de Waele C, Jaubert J. Behavioral effects of a deletion in Kcnn2, the gene encoding the SK2 subunit of small-conductance Ca^{2+}-activated K^{+} channels. Neurogenetics. 2008; 9:237–248. [PubMed: 18604572]

Weisz C, Glowatzki E, Fuchs P. The postsynaptic function of type II cochlear afferents. Nature. 2009; 461:1126–9. [PubMed: 19847265]

Xu T, Nie L, Zhang Y, Mo J, Feng W, Wei D, Petrov E, Calisto LE, Kachar B, Beisel KW, Vazquez AE, Yamoah EN. Roles of alternative splicing in the functional properties of inner ear-specific KCNQ4 channels. J Biol Chem. 2007; 282:23899–23909. [PubMed: 17561493]

Yi E, Roux I, Glowatzki E. Dendritic HCN channels shape excitatory postsynaptic potentials at the inner hair cell afferent synapse in the mammalian cochlea. J Neurophysiol. 2010; 103:2532–2543. [PubMed: 20220080]

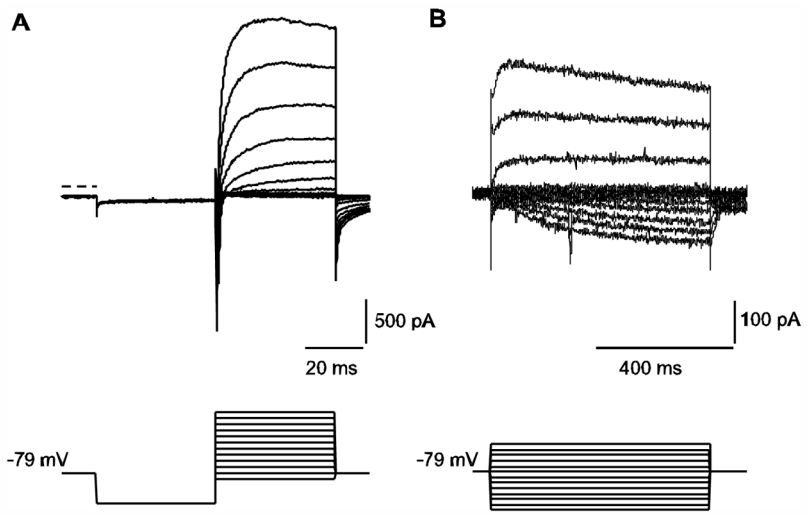

Fig. 1.

Representative whole cell ionic currents in calyx terminals. **A)** A P14 calyx was held at −79 mV and given a hyperpolarizing step to −129 mV followed by a series of depolarizing steps in 10 mV increments between −89 and +21 mV (voltage protocol shown in lower panel). Rapid inward Na^+ currents followed by slowly developing outward K^+ currents are seen at membrane potential steps to −39 mV and above (current traces shown in upper panel). Zero-current level is indicated by the dashed line. **B)** In response to longer duration voltage steps between −149 mV and −29 mV (voltage protocol shown in lower panel), a slowly developing inward current is seen in response to hyperpolarizing steps (P27 calyx).

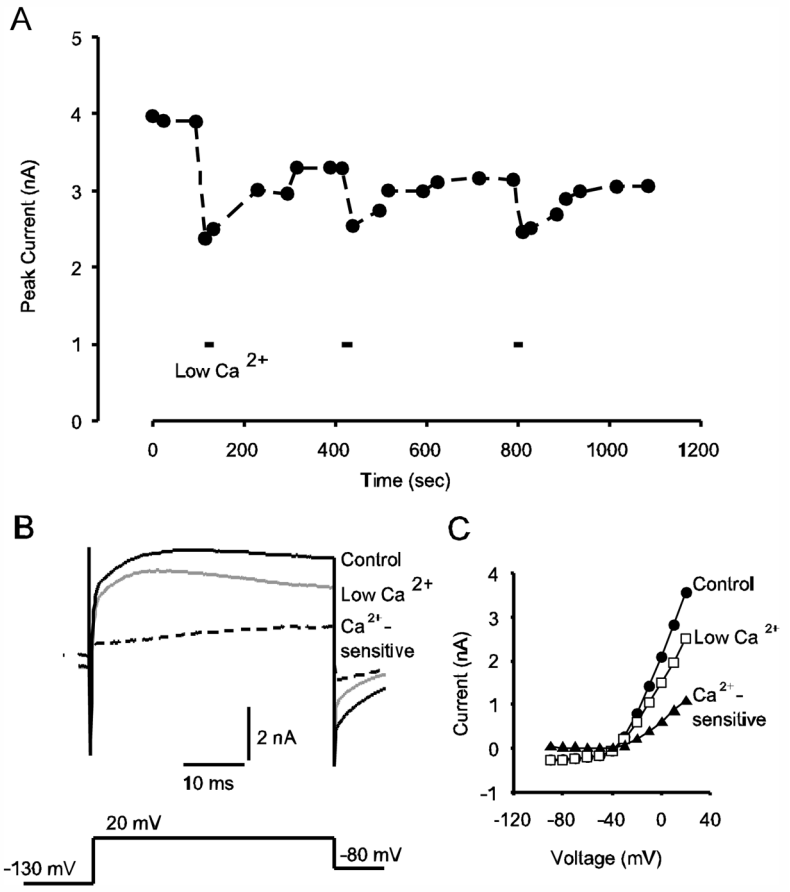

Fig. 2.

Calcium-sensitive currents in calyx terminals. **A)** Peak outward currents measured during depolarizing voltage steps to +20 mV are plotted versus time for a P15 calyx exposed to three short applications of low Ca^{2+} solution (indicated by bars). Outward currents showed a partial recovery after each application. The gradual decline in outward current is likely due to rundown (see Methods). **B)** Currents in response to a voltage step to +20 mV are shown for control and low Ca^{2+} condition in a P15 calyx. The membrane potential was held at −80 mV and stepped to −130 mV for 40 ms before stepping from −90 mV to +20 mV in 10 mV increments (only part of protocol is shown, for complete voltage protocol refer to Fig. 1A). The same voltage protocol was used in figures 3–5. The Ca^{2+}-sensitive component, obtained by subtracting the current in low Ca^{2+} from control is also shown (dashed line). Zero-current level is indicated by the dotted line. **C)** Current-voltage (I-V) plots for steady-state currents at a series of potentials for control (filled circles) and low Ca^{2+} (open squares) for the cell shown in **B**. The subtracted currents (triangles) represent the current sensitive to Ca^{2+} removal and activate above ~ −40 mV

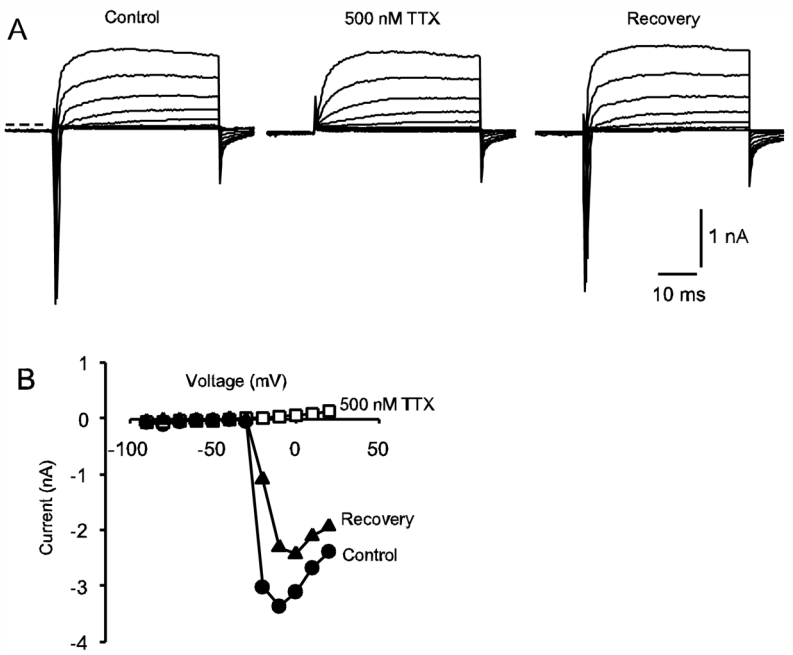

Fig. 3.

Transient inward currents in calyx terminals. **A)** Typical inward and outward currents in response to the standard voltage protocol are shown in a P8 calyx. The transient inward currents were abolished by application of TTX confirming their identity as Na^+ currents. Currents are shown under control conditions (left), following application of 500 nM TTX (middle) and following washout of the drug (right). Zero-current potential is indicated by the dashed line. The membrane potential was held at −80 mV and stepped to −130 mV for 40 ms before stepping to test potentials between −90 and +20 mV. **B)** I-V plot shows peak inward currents for the cell shown in **A**, control (filled circles), 500 nM TTX (unfilled squares) and recovery (filled triangles). Currents were measured within the first 3 milliseconds following the voltage step

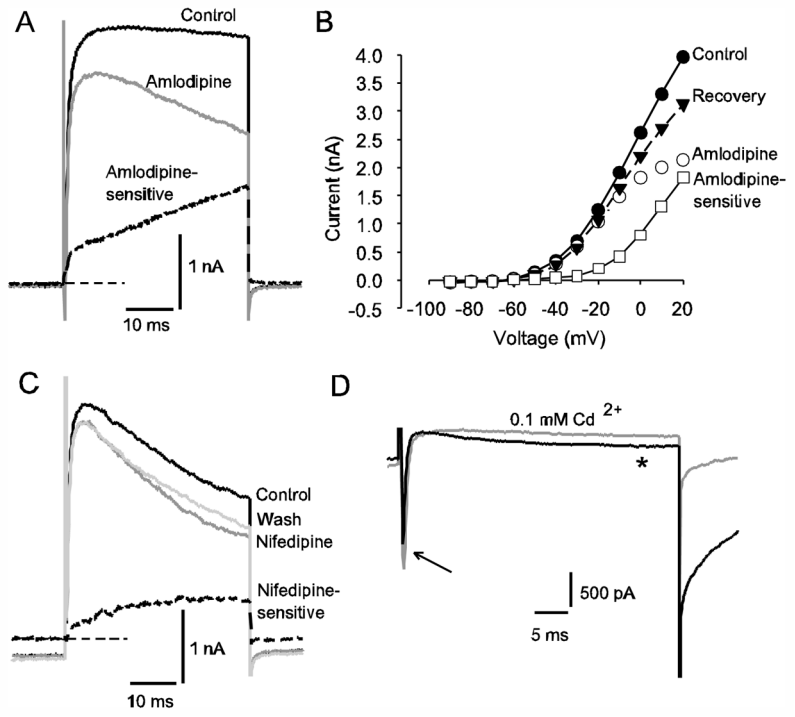

Fig. 4.

Evidence for an L-type Ca^{2+} current in calyx terminals. **A)** Control current, current after application of 7 μM amlodipine and the amlodipine-sensitive current obtained by subtraction (dashed line) are shown in a P30 calyx in response to a depolarizing voltage step to +20 mV. Zero-current level is indicated by thin dashed line. **B)** The I-V plot shows steady-state currents at a series of voltage steps for the same cell as in **A**. Control currents (filled circles) currents in 7 μM amlodipine (open circles), the amlodipine-sensitive current obtained by subtraction (open squares) and currents following drug washout (filled triangles) are shown. **C)** Nifedipine application reduced outward current in a P33 calyx. Control current, current in the presence of 20 μM nifedipine (dark grey line) and a partial recovery following washout (light grey line) are shown in response to a +21 mV depolarizing voltage step. The nifedipine-sensitive current is shown by the dashed line. Zero-current level is indicated by the thin dashed line. **D)** Effect of Cd^{2+} on slow inward currents in a calyx terminal (P28). Electrode solution contained Cs^{+} in place of K^{+}. Superimposed currents following a voltage step to −10 mV are shown and include a rapid transient I_{Na} (arrow) followed by a slowly activating inward current (*). The slow inward current and inward tail current after the test step were greatly reduced in the presence of 100 μM $CdCl_2$ (grey current trace), indicating the presence of Ca^{2+} current

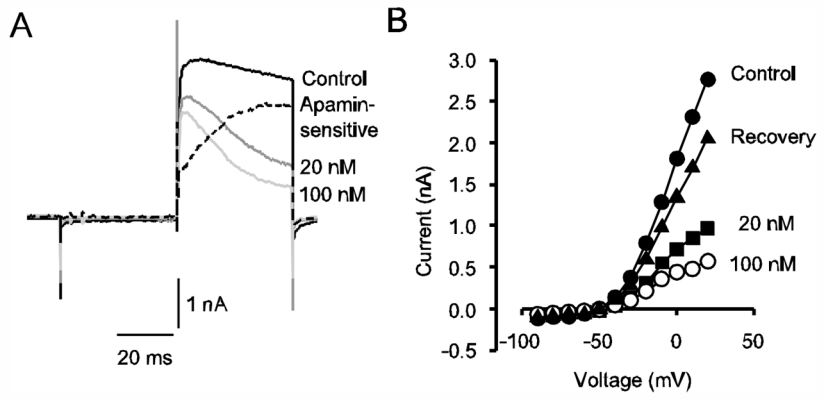

Fig. 5.

Apamin blocks a slowly activating outward current in calyces. **A)** Control current and currents following application of 20 and 100 nM apamin to a P24 calyx are shown. The apamin-sensitive current was obtained by subtracting the current remaining in 100 nM apamin from the control current and is also shown (dashed line). Zero-current level is indicated by the dotted line. **B)** I-V plot shows steady state currents at different voltages for control currents (filled circles), currents in 20 nM apamin (filled squares), 100 nM apamin (unfilled circles) and recovery (filled triangles)

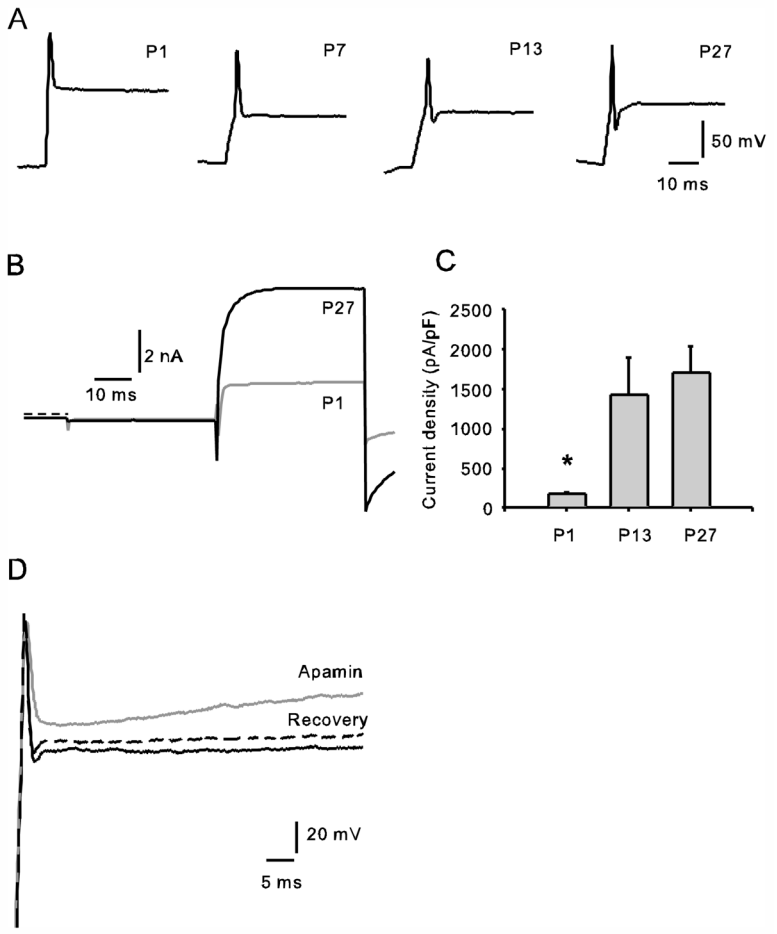

Fig. 6.

Development of ionic currents and action potentials in calyces. **A)** Representative action potentials recorded from P1, P7, P13 and P27 calyces are shown. Cells were given a hyperpolarizing current injection of ~ 1.5 nA followed by a 600 pA step in order to evoke action potentials. An AHP was evident following spikes at P13 and P27, but was not seen at P1 or P7. **B)** Superimposed currents in voltage clamp from P1 and P27 calyces. Both cells showed similar transient inward Na^+ currents followed by outward K^+ currents following a voltage step to +20 mV, but the size of the outward current was much larger at P27. Zero-current level is indicated by the dashed line. **C)** Peak outward currents, measured at +20 mV, were normalized to whole cell capacitance at 3 different postnatal ages. Mean values ± SEM are shown for P1 (n = 3), P13 (n = 9) and P27 (n = 9) calyx terminals. Outward current density was statistically significantly different at P1 and P27 (unpaired t-test, $P < 0.05$). **D)** Superimposed voltage responses to a 600 pA depolarizing current pulse following membrane hyperpolarization are shown for control (black), following application of 100 nM apamin (grey) and recovery following washout of the drug (dashed line) in a P16 calyx terminal. Initial zero-current potential was −42 mV